Aesthetic Effects on Granite of Adding Nanoparticle TiO$_2$ to Si-Based Consolidants (Ethyl Silicate or Nano-Sized Silica)

J. Santiago Pozo-Antonio [1,*] **, Daniel Noya** [2] **and Cristina Montojo** [2]

1   Departamento de Enxeñaría dos Recursos Naturais e Medio Ambiente. Universidade de Vigo, 36310 Vigo, Spain

2   Escola Superior de Conservación e Restauración de Bens Culturais de Galicia, 36002 Pontevedra, Spain; danielnoyapintos@gmail.com (D.N.); cmontojo@edu.xunta.gal (C.M.)

*   Correspondence: ipozo@uvigo.es; Tel.: +34-986-814-077

Abstract: Considering that consolidant products are commonly used in the cultural heritage field and the titanium oxide nanoparticles (TiO$_2$) have been used to develop photocatalyst films to induce self-cleaning property, the scientific research on consolidants doped with TiO$_2$ is justified. However, the addition of TiO$_2$ can affect to the physical properties of the cultural heritage object, questioning the adequacy of the procedure. In this paper, we evaluated the influence of nanoparticle TiO$_2$ addition to two different commercial consolidant products (ethyl silicate or nano-sized silica) on the appearance and the color of a granite and the penetration through its fissure system. The stone was previously subjected to high temperature simulating the effect of a fire and the subsequent tap water jet to cool down. Therefore, different concentrations of nanocrystalline TiO$_2$ (0.5, 1, and 3 wt %) were considered. The different compositions were also studied considering the compactness, the extent and the thickness of the superficial xerogel coating, and as well the penetration of the consolidant. The minimal TiO$_2$ concentration tested (0.5 wt %) implied a low-medium risk of incompatibility as an intervention in cultural heritage field, because its low-medium potential as inducer of visible color changes of the granite surface. Regardless of the TiO$_2$ content, the nano-sized silica induced surface xerogel coatings more compact and continue than those formed in the ethyl silicate coated surfaces. Higher penetration rates were identified in the granite treated with nano-sized silica colloidal solution, while ethyl silicate was only found in the first few μm. It was found that penetration could depend on the application procedure, the solvent of the consolidant and the silica particle size. The TiO$_2$ addition reduced the penetration of the nano-sized silica consolidant.

Keywords: titanium oxide; nanoparticle; conservation; cleaning; photocatalysis; nanoparticle concentration; physical change

1. Introduction

In the conservation of the cultural heritage field, the application of consolidant products seeks the strengthening of the deteriorated surfaces with historic and artistic value and subsequently the mitigation of their disintegration. In stones belonging to cultural heritage, deterioration forms—such as sanding, splintering, flaking, etc.—are due to different processes (e.g., fire, abrasion, soluble salts crystallization, etc.) that in many cases cannot be avoided [1]. Considering that consolidation is an irreversible treatment, scientific research is justified to improve the cohesion of the stone surface and slow down its natural deterioration. Commonly, alkoxysilanes, such as tetraethoxysilane (TEOS) products are applied due to their low viscosity and their ability to form siloxane bonds [2]. These products polymerize inside the pore through a sol–gel process obtaining a xerogel, increasing the cohesion

of the deteriorated surface. Cracking occurs as result of the occurred capillary pressure within the gel inside the stone pores [3–5] and the evaporation of the solvent during the drying step upon the gelation process on the outer surface of the capillary network, since the drying front is exposed to ambient atmosphere [6]. Shrinking results from stress due to a meniscus at the liquid–vapor interface, which generates a differential capillary pressure within the gel as the solvent tends to evaporate. In the case of TEOS-based products, cracking also occurred due to the TEOS/organometallic catalyst ratio [7,8]. As one of the most important drawbacks of alkoxysilanes is the trend to form superficial cracking layers and the lack of penetration through the fissure system of the stone [3–5], different strategies have been adopted in the recent years in order to obtain the highest product penetration avoiding surface accumulation, such as the application of nanotechnology to the consolidants' manufacturing [9].

Nanotechnology allows the incorporation of silicon dioxide nanoparticles to consolidants to enhance the dispersion stability and the penetration through fissures [9–11]. Zendri et al. [11] working with a colloidal suspension of silica nanoparticles of 10–15 nm, sodium silicate and ethyl silicate with calcium carbonate and quartz, found that these consolidants constitute gels of amorphous silica that after the evaporation of the solvent were transformed into xerogels. These xerogels are made by a disorderly and continuous lattice of silica tetra-coordinated tetrahedrons that constitute rings with 3 at 8 atoms of silicium. Zendri et al. [11] reported that the ethyl silicate has less of a cohesion effect on mortars than sodium silicate and colloidal silica. They found a greater penetration of the colloidal silica which shows lesser dimensions of the particles than those composing the sodium silicate and the ethyl silicate.

Moreover, water-based silica nanoparticles with radius from 55 to 9 nm-dispersions were used by Falchi et al. [12] achieving a penetration depth of 2 mm on Lecce stone. Calcarenites coated with the commercial product Nano Estel from CTS S.L. cured at low relative humidity (40%) showed better effectiveness than those subjected to higher humidity [10]. Nano Estel is an aqueous colloidal solution of nano-size silica particles (10–30 nm). The nano-size silica particles bind among themselves forming a silica gel, similarly to that obtained for ethyl silicate consolidants. La Russa et al. [13] working on the consolidation of Cappadocian ignimbrite cave churches found that Nano Estel induced a lower penetration than the solvent-based tetraethoxysilane (TEOS) products (Estel 1000 and Estel 1100). However, Nano Estel left the stone porous structure unaltered [10].

In addition, nanoparticles have been used to achieve layers on stones, mortars, glasses, etc. favoring the self-cleaning and water-repelling [9,14–16]. Among these nanoparticles, TiO_2 is widely used for the destruction of organic pollutants and to avoid biological colonization [17–19]. TiO_2 shows the following characteristics: high photoactivity, good stability, low cost, and low toxicity [20,21]. TiO_2 absorbs UV radiation producing free radicals that react with organic matter on the surfaces through oxidation into H_2O and CO_2 [16,22]. TiO_2 is shown as three crystalline structures: rutile, anatase, and brookite, being the first two forms as the most suitable for photocatalysis [23]. The photooxidation of organic matter has been evaluated in different construction materials such as bricks [24], stone [18,25], and mortars based in different binders [19,26,27]. Most of the research focused on self-cleaning has been made using the TiO_2 product as a coating [21,26].

Therefore, nowadays, the scientific research on the achievement of products inducing simultaneously consolidation, self-cleaning, and water-repelling of stones belonging to cultural heritage is plenty justified. The addition of TiO_2 nanoparticles to commercial consolidant products could be a possibility in order to reach together the advantages of both products; however, an excessive nanoparticle content could induce by-effects such as color modifications that can jeopardize the effect of the consolidant applied on cultural heritage surfaces. As was stated by the deontological code of cultural heritage conservation expressed in the Venice charter [28], a conservation treatment should not modify the properties of the treated materials, such as the color. Spectrophotometry plays an important role in the field of architectural heritage conservation. In the specific case of the application of a consolidant product for strengthening and protecting building stones, a colorimetric study of its effects can quantify the degree to which the chromaticity and lightness of the material has changed,

and whether this change is aesthetically significant. Thus, this research is focused on the influence of the introduction of different concentration of TiO_2 nanoparticles (0.5, 1, and 3 wt %) in commercial consolidants on the appearance and the color of a granitic surface coated in order to determine the suitable TiO_2 content for each consolidant product. Moreover, two different compositions of consolidant products (ethyl silicate or nano-sized silica dispersion) were studied in order to identify the composition most suitable to be used. The microtexture of the consolidant layer on the surface was studied by scanning electron microscopy with energy dispersive X-ray spectrometry. Previously to the consolidant application, samples were subjected to three heating cycles composed each one by 12 h at 500 °C and cooled down to room temperature using tap water jet, simulating the effect caused by firefighters' intervention in a fire.

2. Materials and Methods

2.1. Stone

The selected stone was the commercially called granite, Rodas (Figure 1a). Mineralogically, it shows 25.60% quartz, 30.73% albite, 26.43% microcline, 11.65% muscovite, 5.70% biotite, and 0.20% accessory minerals (apatite, zircon, rutile, sillimanite, chlorite, and opaque minerals) [29]. This yellowish granite belonging to the alkaline granites from the Variscan age sometimes shows flow orientations due to the existence of oxyhydroxylated iron forms of low or no crystallinity filling the fissures [29–32]. The porosity accessible to water of Rodas granite is 6.50 ± 0.2 % following [33]. The high open porosity allows an easy carving and therefore it is usually found in ancient architectural constructions in the NW Iberian Peninsula. Following [34] the pore size distribution by mercury intrusion porosimetry (MIP) with a Fison Instruments Pascal Porosimeter, reported that this granite had four pores families: (i) the main one pore family corresponds to that with diameters between 0.1–5 μm; (ii) coarser pores with diameters 300–100 μm; (iii) pores with diameters between 10–50 μm; and (iv) finer pores with diameters 0.1–0.06 μm. In addition, 80% of the porous volume corresponds to pore diameters greater than 1 μm. It is also obtained that the volume of pores in the capillary absorption range (0.1–100 μm according to [35]) constitutes 97% of the total porous volume, mostly in the diameter range between 1–100 μm.

In order to start with the experiment, 27 4 cm × 4 cm × 4 cm cubes with dish cutting finish were cut. Three of these cubes were reserved as reference samples.

Prior to the consolidant application, samples were subjected to 500 °C during 12 h and subsequently, they were cooled by tap water jet and placed at laboratory conditions (15 ± 5 °C and RH 60 ± 10%) during two days. This cycle was repeated three times. After the heating cycles, the surface of the granite showed a slight reddening mainly of the leucocratic minerals (K-feldspar and plagioclase) (Figure 1b) comparatively to the stone without heating due to the transformation to hematite of the Fe oxyhydroxides present into the granite fissures, as was reported in [36], working in a petroglyph site with similar mineralogy and texture to this Rodas granite. In addition, typical appearance of the granite forming minerals was observed (Figure 1b): conchoidal fracture of translucid quartz grains, black exfoliation planes of biotite and whitish coloration of feldspar grains despite as was reported, areas of the leucocratic minerals showed a reddish coloration due to the hematite filling fissures as a consequence of the heating.

A surface fragments (approximately 1 cm × 1 cm × 1 cm) of the granite surfaces subjected to 500 °C was embedded in resin and the polished cross section was observed by Scanning Electron Microscopy (SEM) using a Philips XL30 (Amsterdam, The Netherland) coupled with an energy dispersive X-ray spectrometry (EDS) (Oxford Inca Energy 300 SEM, Oxfordshire, UK) in secondary electrons (SE) and backscattered electrons (BSE) modes. Carbon-coated sample were visualized at an accelerating potential of 15–20 kV, a working distance of 9–11 mm and specimen current of 60 mA. In Figure 1c,d are shown micrographs taken by SEM with the corresponding EDS spectra. In addition to the main forming minerals (biotite: EDS1; K-feldspar: EDS2; quartz: EDS3; Na-plagioclase: EDS4) and the

accessory mineral apatite (EDS5). Moreover, Al and Si-rich deposits filling fissures were also detected (EDS6). These deposits can be kaolinite precursors that are usually found in Variscan granite used in heritage construction [37] and they are result from chemical weathering, specifically hydrolysis of feldspar and micas [31,32,38,39].
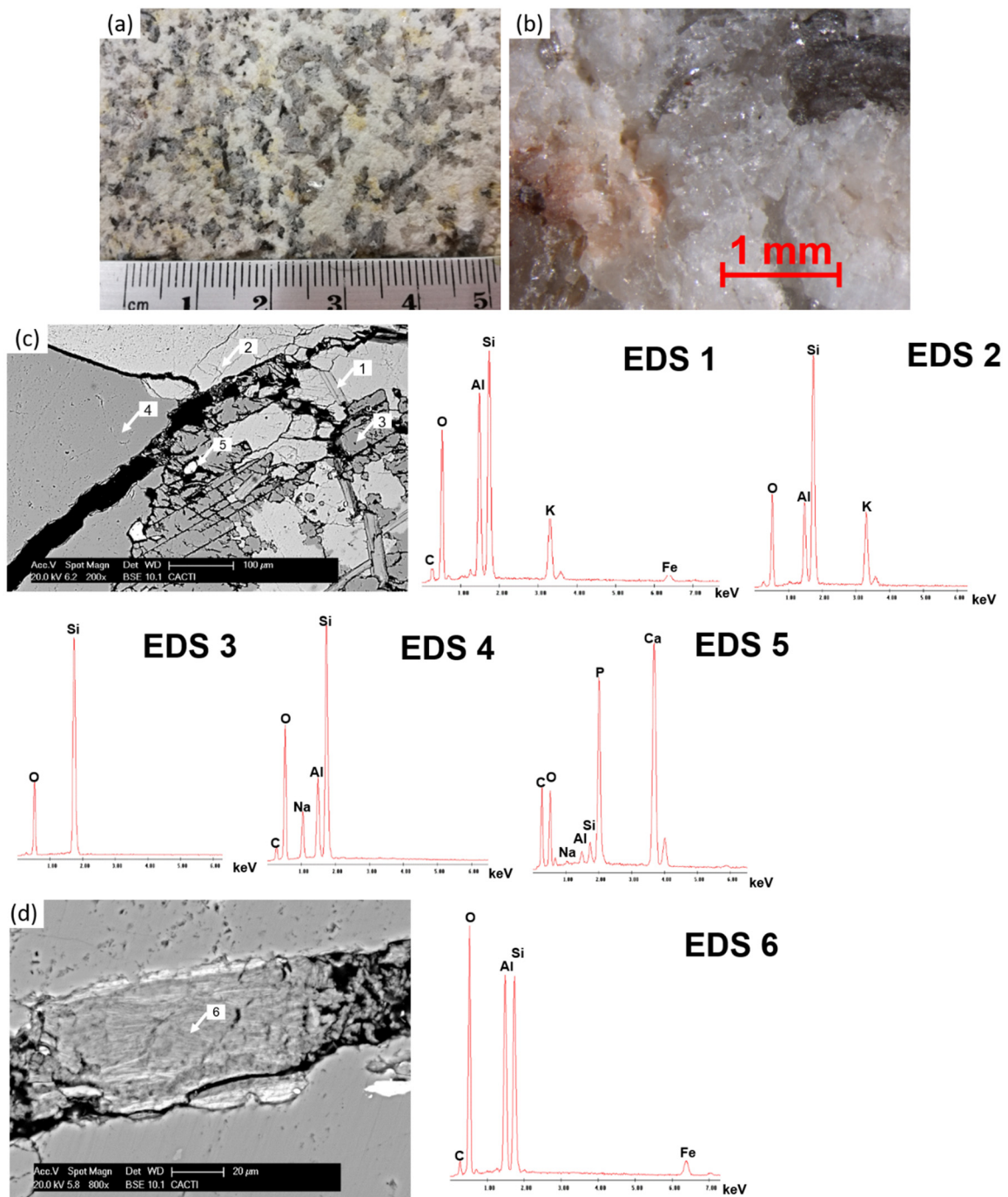

Figure 1. Rodas granite. (**a**) Digital photograph; (**b**) Micrograph taken with stereomicroscopy. (**c**,**d**) SEM micrographs of a polished cross section of the reference granite and EDS spectra of the granite. EDS1: biotite, EDS2: K feldspar, EDS3: quartz, EDS4: Na plagioclase, EDS5: apatite, EDS6: Al-, Si-, and Fe-rich deposits filling fissures.

2.2. Consolidants

The commercial consolidant products provided by CTS España S.L [40] were:

- Estel 1000® (hereinafter E) is composed of 75 wt % ethyl silicate oligomers (also containing 1% dibutyltin dilaurate as catalyst) and 25 wt % White Spirit D40 (a mixture of aliphatic hydrocarbons having a boiling point of 145–250 °C). SiO_2 content of 30 wt %. It was applied undiluted.
- Nano Estel® (hereinafter N) is an aqueous colloidal solution of nano-size silica particles (10–30 nm). By the manufacturer it is recommended to apply it directly for ruined substrates or at 30 vol % in water for less deteriorated surfaces. Considering the granite was exposed to 500 °C (three cycles), it was directly applied.

2.3. Sample Preparation

The titanium dioxide (TiO_2) used was the same photocatalyst additive used in [41]. It was the product Aeroxide P-25 from Evonik Resource Efficiency GmbH [42]. It consists of nanocrystalline anatase with specific surface area of 50 $m^2 \cdot g^{-1}$. As was reported in [41] nanoparticles were hexagonally shaped rounded with a size about 30 nm.

Commercial consolidants were directly mixed with three different TiO_2 concentrations (0.5, 1, and 3 wt %). Moreover, a condition without TiO_2 addition (0 wt %) was also considered. For each composition, three cubes were coated. Table 1 shows the composition and the acronyms used in the experiment. Before the consolidant application, following [12], ethanol by brushing through a single application was applied on the stone surface in order to reduce the superficial tensions to enhance the penetration. As was reported in [12], the stone surface was covered with Japanese paper.

The products were applied by brushing on the samples through 4 applications. After each application, samples were left to laboratory conditions (18 ± 5 °C and 50% ± 10% RH) during 48 h. After the fourth application, samples were kept air dry (18 ± 5 °C and 50% ± 10% RH) until constant weight (approximately 30 days) in order to ensure the polymerization of the products. However, note that color changes can be observed over longer periods of time and dramatic darkening effects, after five years, can be almost imperceptible. Wheeler [2] reported some researchers focused on TEOS-based products where the turning to the original color in time or after artificial weathering was found.

Three cubes without consolidants (hereinafter 'reference') were also included in the study in order to compare the results of the consolidated samples with those without.

Table 1. Conditions used in the experiment. Acronyms are also depicted.

TiO_2 (wt %)	Estel 1000	Nano Estel
0	E	N
0.5	E0.5%	N0.5%
1	E1%	N1%
3	E3%	N3%

2.4. Analytical Techniques

The coated samples were evaluated by means of stereomicroscopy and color spectrophotometry in order to identify the influence of the addition of TiO_2 nanoparticles in the two commercial consolidants on the appearance and the color of the surface of the coated stone.

Firstly, an initial macroscopic characterization with a stereomicroscope (Nikon SMZ800, Tokyo, Japan) was carried out for all the samples to characterize the consolidant layers doped with TiO_2 nanoparticles in comparison to those without TiO_2 and with the reference granite.

Color characterization of the reference surface and the coated samples using a Minolta portable spectrophotometer model CM-700 (KONICA MINOLTA, Osaka, Japan) equipped with CM-S100w (SpectraMagic™ NX, Osaka, Japan) software. Color was expressed in the CIELAB and CIELCH color

spaces [43]. Therefore, the measured parameters were: lightness (L*) which varies from 0 (absolute black) to 100 (absolute white); a*, representing the redness–greenness range (positive a*: red and negative a*: green); b*, associated with yellowness–blueness spectrum (positive b*: yellow and negative b*: blue). The chroma which is the saturation (C^*_{ab}) was calculated based on a* and b* values as

$$C^*_{ab} = (a^{*2} + b^{*2})^{1/2} \tag{1}$$

Moreover, the hue (h_{ab}) was computed as

$$h_{ab} = \tan^{-1}(b^*/a^*) \tag{2}$$

Color measurements were made in specular component included (SCI) mode, for a spot diameter of 8 mm with diffuse illumination by means of xenon flash arc lamp and 10 nm diffuse bandwidth, using illuminant D65 at observer angle 10°. Following [44] a total of 20 random readings were made for each surface (n = 60 measurements).

Afterwards, partial ΔL^*, Δa^*, Δb^*, ΔC^*_{ab}, and ΔH^* color coordinates differences and the global color change (ΔE^*_{ab}) were calculated following [43], taking as reference the color of the reference granite. The global color change (ΔE^*_{ab}) was computed as

$$\Delta E^*_{ab} = (\Delta L^{*2} + \Delta a^{*2} + \Delta b^{*2})^{1/2} \tag{3}$$

Moreover, in order to study the microtexture and compactness of the consolidant layer, 1 cm × 1 cm × 1 cm fragments of the coated surfaces were C-sputtered and were observed by SEM-EDS using a FEI Quanta 200 (Eindhoven, The Netherlands) with secondary electron (SE) and backscattered electrons (BSE) detectors. After observation, the same samples were embedded with an epoxy resin (EpoThin 2 Epoxy Resin and EpoThin 2 Epoxy Hardener) to which was added a conductive filler rich in Ni in rounded molds (3.5 cm diameter). Once hard, a transversal cut was performed to obtain specimens with 1 cm-width. These specimens were polished and C-coated to be visualized using SEM-EDS. Applied as optimum conditions of observation were an accelerating potential of 20 kV, a working distance of 10 mm and a specimen current of ~60 mA.

3. Results

Stereomicroscopy allowed the characterization of the appearance of the surfaces coated with the different consolidants by themselves (0% TiO_2) and mixed with the different TiO_2 nanoparticles concentration (0.5%, 1%, and 3%) in order to identify the aesthetical changes (Estel 1000 coating: Figure 2 and Nano Estel coatings: Figure 3). For the surfaces coated with the consolidants without TiO_2, at naked eye it was possible to identify a darkening of the surface (Figure 2a and Figure 3a). In general terms, as the higher the TiO_2 concentration, the higher the aesthetical effect, because white deposits in the superficial fissures and voids were found (Figures 2 and 3). The white deposits showed the typical cracks identified by scanning electron microscopy in the commercial products containing tetraethoxysilane [4]. Comparing between consolidants, for the higher TiO_2 nanoparticles concentration (1% and 3%), the surfaces showed similar appearance (Figure 2c,d and Figure 3c,d). However, the most notable difference was found on the surfaces coated with 0.5% TiO_2, because, despite cracks also being found on the coatings, a more continuous layer was detected on the surface when Nano Estel was used as consolidant (Figure 3b) while on the surface coated with Estel 1000, accumulation of product was found in fissures and voids of the surfaces (Figure 2b).
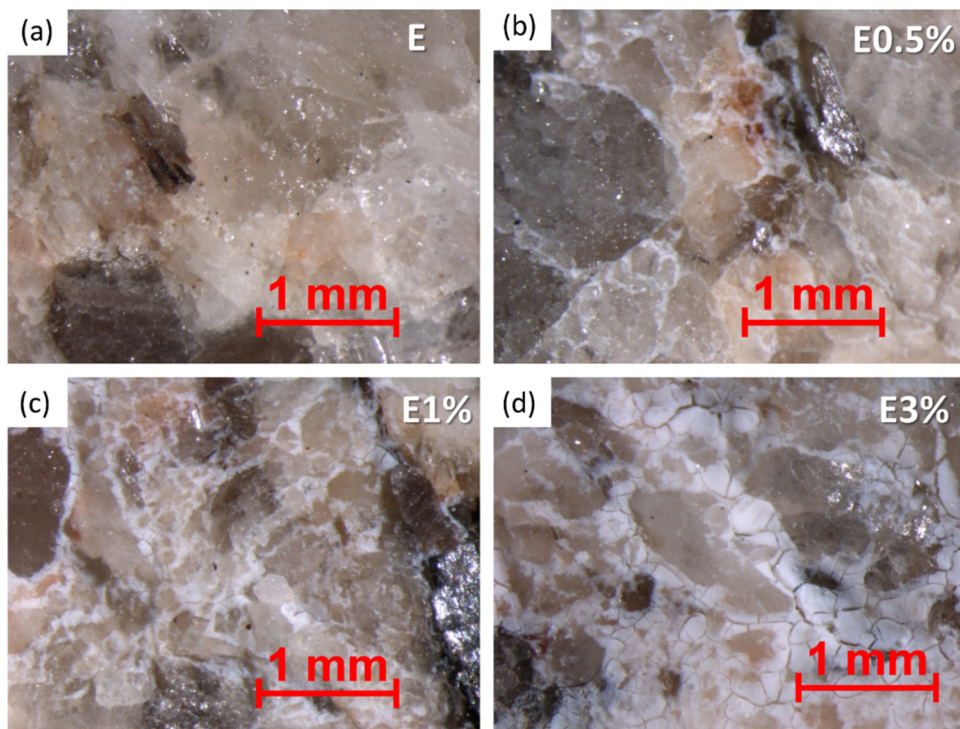
Figure 2. Micrographs taken with stereomicroscopy of the surfaces covered with the ethyl silicate-based consolidant Estel 1000 and the different TiO_2 nanoparticles concentration (**a**: 0%; **b**: 0.5%, **c**: 1%, and **d**: 3%). Check Table 1 to understand the acronyms.
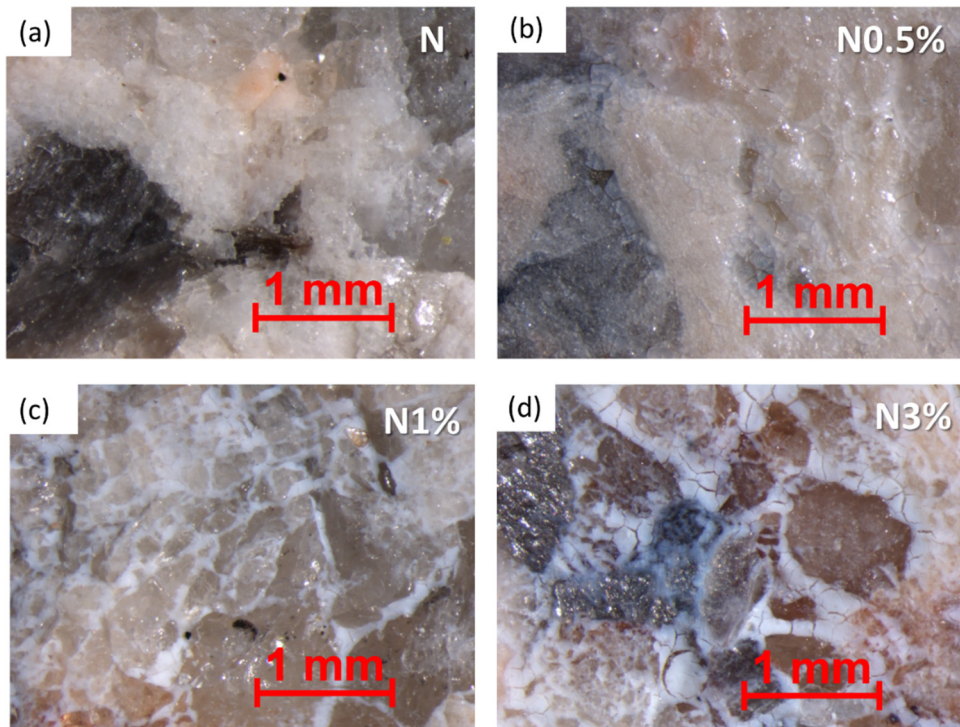

Figure 3. Micrographs taken with stereomicroscopy of the surfaces covered with the nano-sized silica-based consolidant Nano Estel and the different TiO_2 nanoparticles concentration (**a**: 0%; **b**: 0.5%, **c**: 1%, and **d**: 3%). Check Table 1 to understand the acronym.

Considering the scatter L*-C*$_{ab}$ plots (Figure 4), the coated samples regardless of the consolidant composition and the TiO$_2$ concentration showed a color with higher dispersion than the uncoated surfaces. The consolidants (without TiO$_2$) induced a C*$_{ab}$ increase and a slight L* reduction. Addition of the 0.5% and 1% TiO$_2$ to the consolidants also caused a reduction of the L* and a slight increase of the C*$_{ab}$ (less intense than those found for the samples coated without TiO$_2$ addition). However, the application of the highest TiO$_2$ concentration tested (3%) caused a L* increase and a C*$_{ab}$ decrease.
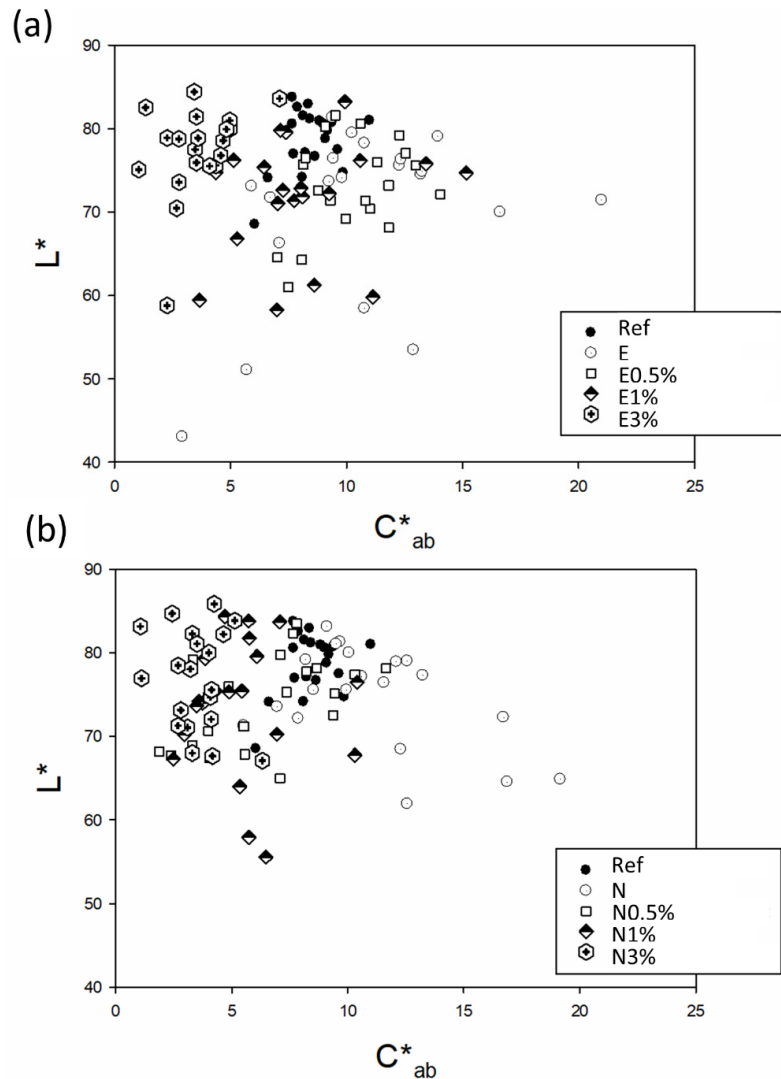

Figure 4. L* and C*$_{ab}$—scatter plots of the surfaces treated with the two consolidants and different nanoparticles TiO$_2$ concentrations. Measurements for the reference uncoated granite (Ref) and the coated surface only with the consolidant are also shown. (**a**) Estel 1000 samples; (**b**) Nano Estel samples. Check Table 1 to understand the acronyms.

The most affected parameter was L* for the surfaces coated only with Estel 1000 (E) and for the conditions E0.5%, E1% (Table 2). Considering the rest of the conditions, b* was clearly the parameter most affected by the color change in the samples with the highest TiO$_2$ concentrations (E3% and N3%), while the other conditions, showed changes of L* and b* very close (less than 1 CIELAB unit). Attending to the trend of each parameter, L* showed decreases with exception of the surfaces with the highest TiO$_2$ concentration: L* decreases reflects a darkening of the surface. The b* parameter in the surfaces coated with the consolidant without TiO$_2$ exhibited increases suggesting a yellowing of the surface due to the consolidant application. However, in the coated surfaces with TiO$_2$, except

for E0.5%, b* showed decreases; the higher the TiO_2 concentration, the higher the reduction of b*. This change shows a loss of the yellow coloration, which is a typical feature of this granite. Although the changes were less intense than for the b*, a* also showed variations; a* increases were detected in the surfaces of E, E0.5%, E1%, N and N0.5%. These increases represent a reddening in coloration. However, for the surfaces coated with the higher TiO_2 concentrations, a* showed decreases due to the loss of the red color. As result of these changes, C^*_{ab} experimented increases for the E, E0.5% and the N, while the rest of the samples showed decreases, which are related to a paling effect. Regarding the hue, only the surfaces coated with 3% TiO_2 mixed with Nano Estel (N3%) showed higher values of three CIELAB units.

Attending to the global color change (ΔE^*_{ab}), only the sample with Nano Estel (N) showed a value lower than 3.5 CIELAB unit (Figure 5) which is the threshold from which a color change is visible to a non-expert observer [45]. Unexpectedly, Estel1000 (E) caused the highest global color change (ΔE^*_{ab} = 7.46 CIELAB units). Considering the samples with TiO_2, for those with 0.5% and 1% TiO_2, the mixture with Estel 1000 (E0.5% and E1%) showed higher global color changes than their counterparts with Nano Estel. However, for the sample of Nano Estel with the highest TiO_2 concentration (N3%), the ΔE^*_{ab} was higher than that computed for E3% in almost two CIELAB units. In order to evaluate the potential of these products as inducers of harmful effects, the incompatibility assessment rate proposed in [46] in three levels of risk was used: low risk (ΔE^*_{ab} < 3), medium risk ($3 < \Delta E^*_{ab} < 5$) and high risk (ΔE^*_{ab} > 5). Therefore, the application of Nano Estel by itself and the mixture of both consolidants with 0.5% TiO_2 induced medium risks ($3 < \Delta E^*_{ab} < 5$), while the rest of interventions all induced high risk (ΔE^*_{ab} > 5).

Table 2. Colorimetric variations ΔL^*, Δa^*, Δb^*, ΔC^*_{ab}, and ΔH^* (CIELAB units) of the treated surfaces considering the color of the surface before to be treated as the reference, N = 60.

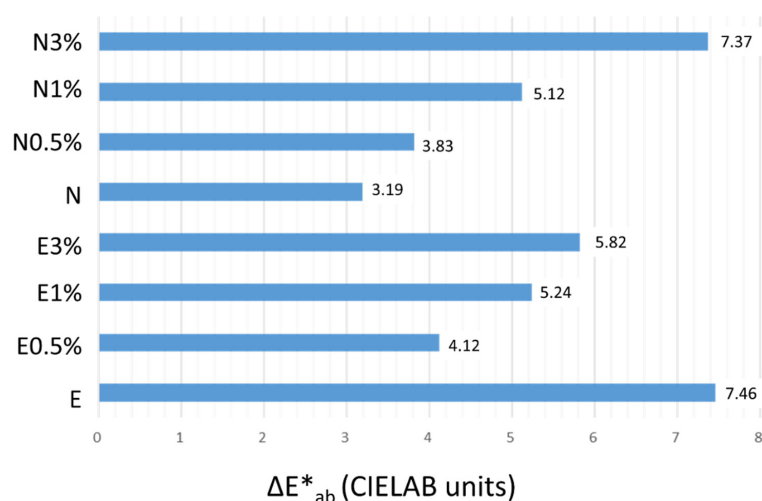|	ΔL^*	Δa^*	Δb^*	ΔC^*_{ab}	ΔH^*
E	−7.33	0.01	1.37	1.28	0.51
E0.5%	−3.77	1.20	1.12	1.53	−0.70
E1%	−5.16	0.43	−0.85	−0.58	−0.74
E3%	0.55	−1.10	−5.69	−5.10	1.97
N	−2.13	1.03	2.15	2.43	0.08
N0.5%	−2.71	0.16	−2.71	−2.24	−1.60
N1%	−3.32	−0.18	−3.90	−3.25	−1.90
N3%	0.05	−0.95	−7.31	−5.21	7.55

Figure 5. Global color change (ΔE^*_{ab}) of the treated surfaces considering the color of the surface before to be treated as the reference.

SEM observation of the surfaces allowed the identification of xerogel coatings (Figures 6 and 7). Those found on the Nano Estel samples, regardless the TiO_2 content, showed higher extent and compactness (Figures 6b and 7b,d) comparatively to those on the Estel 1000 treated surfaces Figures 6a and 7a,c). Attending the consolidants without nanoparticles (Figure 6), despite both consolidants showed crack xerogel coatings on the surfaces, the distribution and morphology of this layer was different considering the consolidant applied. Estel 1000 created a discontinuous less cracked coating on the surface (Figure 6a,c). However, for the sample coated with Nano Estel a more continuous layer was identified (Figure 6b,d).
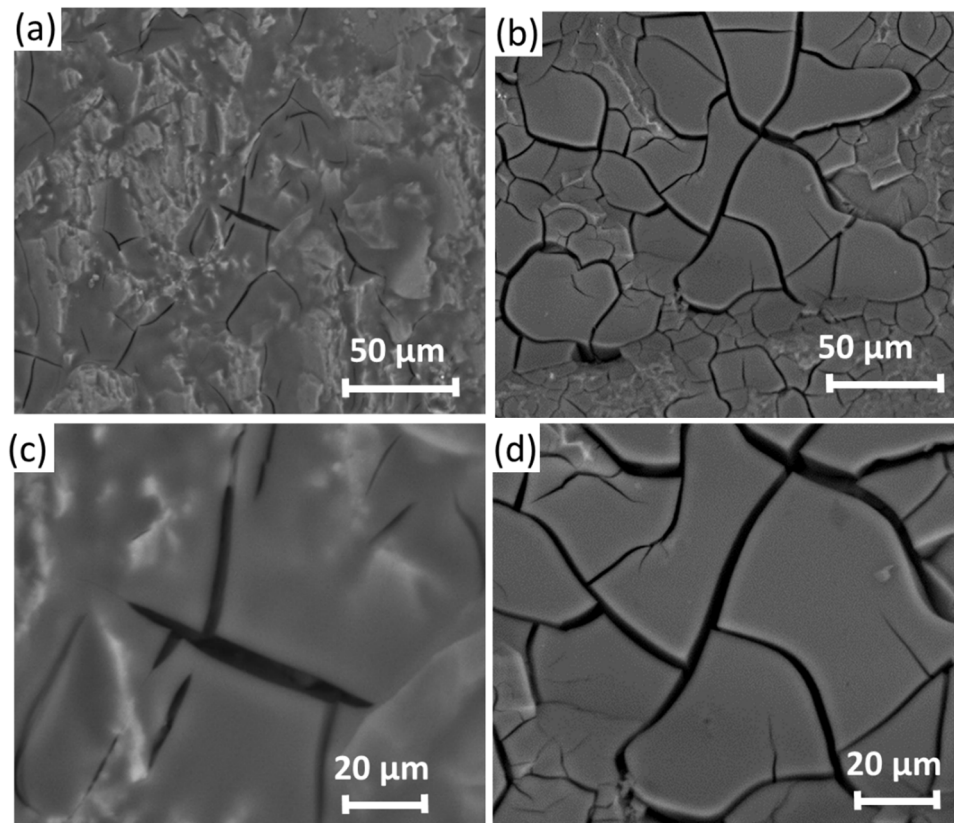

Figure 6. SEM micrographs of the surfaces treated only with the consolidant products. (**a**,**c**) Estel 1000. (**b**,**d**) Nano Estel.

Attending to the TiO_2 addition, SEM-EDS allowed the identification of the Ti-rich nanoparticles embedded in the Si-rich matrix belonging to the consolidant products (Figure 7a,b and EDS1). In terms of compactness, a notable difference was observed considering the consolidant used: Estel 1000 consolidant with TiO_2 showed a less compact layer on the granite surface than those detected on the samples coated with Nano Estel (Figure 7).

SEM observations of the polished cross sections of the samples coated with the consolidants without TiO_2 addition allowed the identification of the penetration rate for both products in the Rodas granite; consolidant products filling fissures were identified through their Si-rich composition (Figure 8): in Figure 8b, EDS spectra allowed the identification of Estel 1000 (Figure 8, EDS 1) on a Na plagioclase (Figure 8, EDS 2) surface. Moreover, compositional maps (Figure 8d,e) showed the penetration of the consolidant into the fissures distinguishing between fissures filled with Si-rich consolidant (Figure 8d) and the C rich resin used in the sample preparation (Figure 8e). Higher penetration rates were identified on the samples coated with Nano Estel (Figure 8c,e) than those found on the sample coated with Estel 1000 (Figure 8a,b). In the Nano Estel-treated sample, consolidant was

found up 200 μm in depth, while on the Estel 1000-treated surface, the consolidating effect was only found in a few μm in depth.
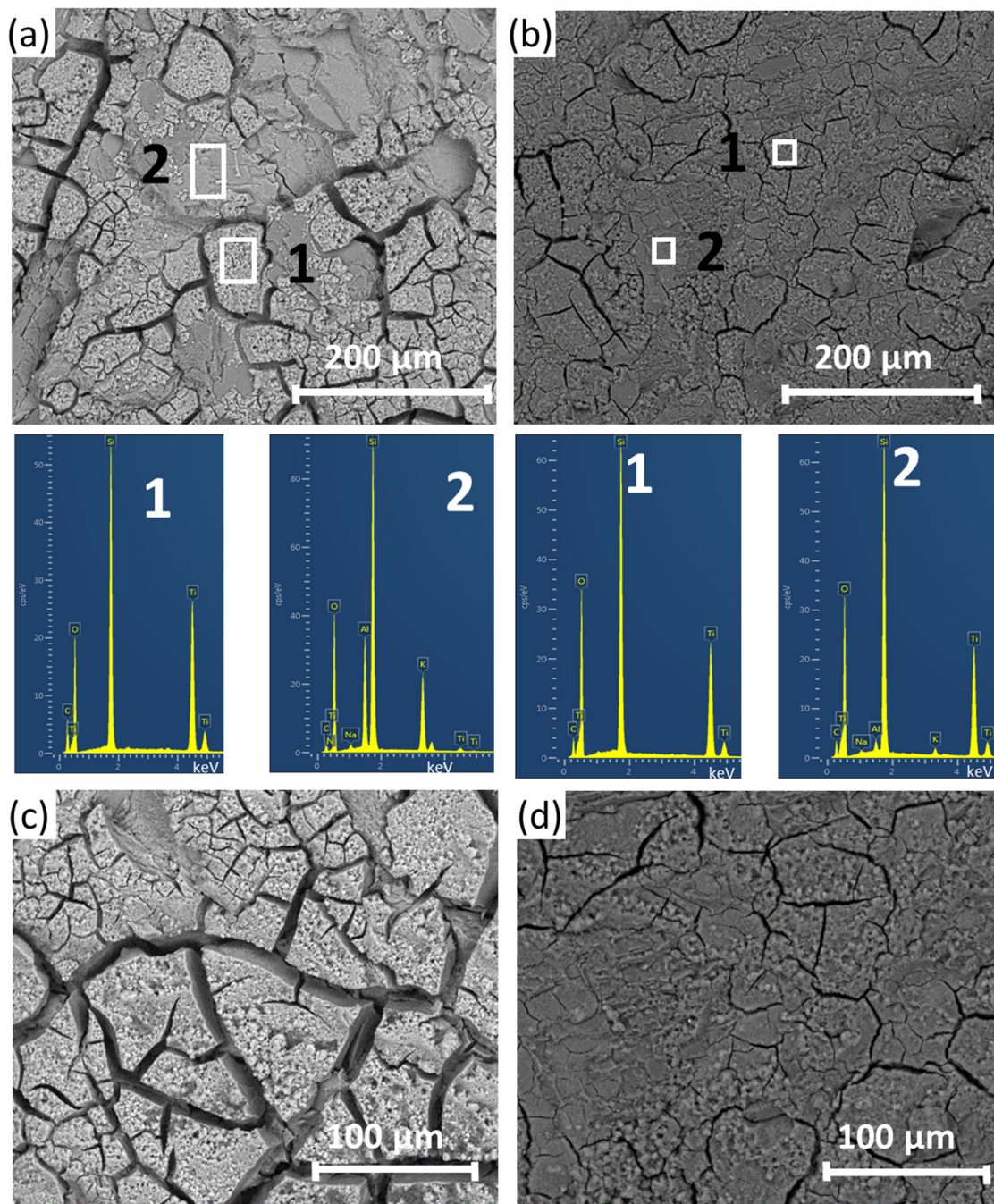

Figure 7. SEM micrographs of the surfaces treated the consolidant products and 3 wt % of TiO_2 nanoparticles concentration. (**a,c**) Estel 1000. (**b,d**) Nano Estel.

SEM micrographs of the polished cross sections from the surfaces with TiO_2 doped consolidants, suggested that the addition of nanoparticles TiO_2 to the Estel 1000 did not induce any change in the penetration rate (Figure 9a,b) since this consolidant without TiO_2 did not show already a clear penetration. However, the TiO_2 addition to Nano Estel affected its penetration rate (Figure 9c,d). In fact, the doped Nano Estel consolidant with the highest wt % TiO_2 showed a penetration reduction of 90% (Figure 9c,d). The highest penetration reduction was detected in the sample coated with the highest TiO_2 concentration (N3%). However, it should be mentioned that the absence of Ti in the EDS spectra of the consolidant into the stone fissures suggested that the TiO_2 nanoparticles were retained on the superficial coating (Figure 9d, EDS 1-3).
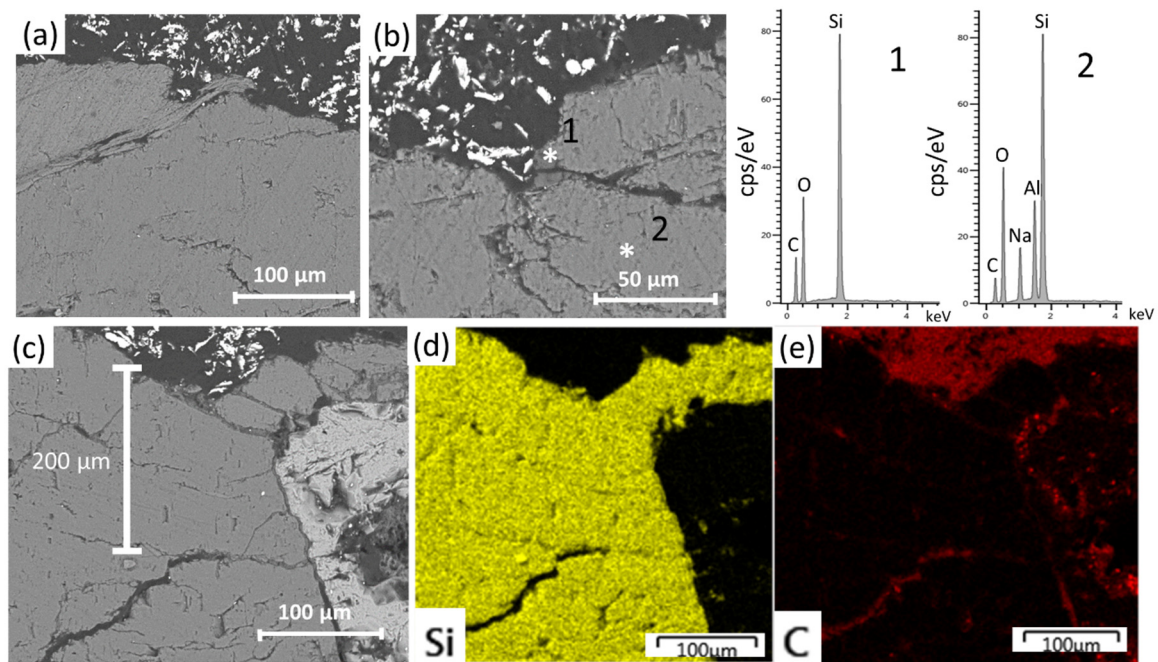

Figure 8. SEM micrographs of the polished cross sections from the surfaces treated with consolidant products without TiO_2 nanoparticles. (**a**,**b**): Estel 1000-treated surface, (b) is accompanied with the EDS spectra. (**c**–**e**): Nano Estel-treated surface. (**d**) Si compositional map. (**e**) C compositional map.

The Ti-rich consolidant coatings formed by agglomerates on the surfaces were thicker on the Nano Estel treated surfaces (Figure 9c) than those found on their counterparts with Estel 1000 (Figure 9a).
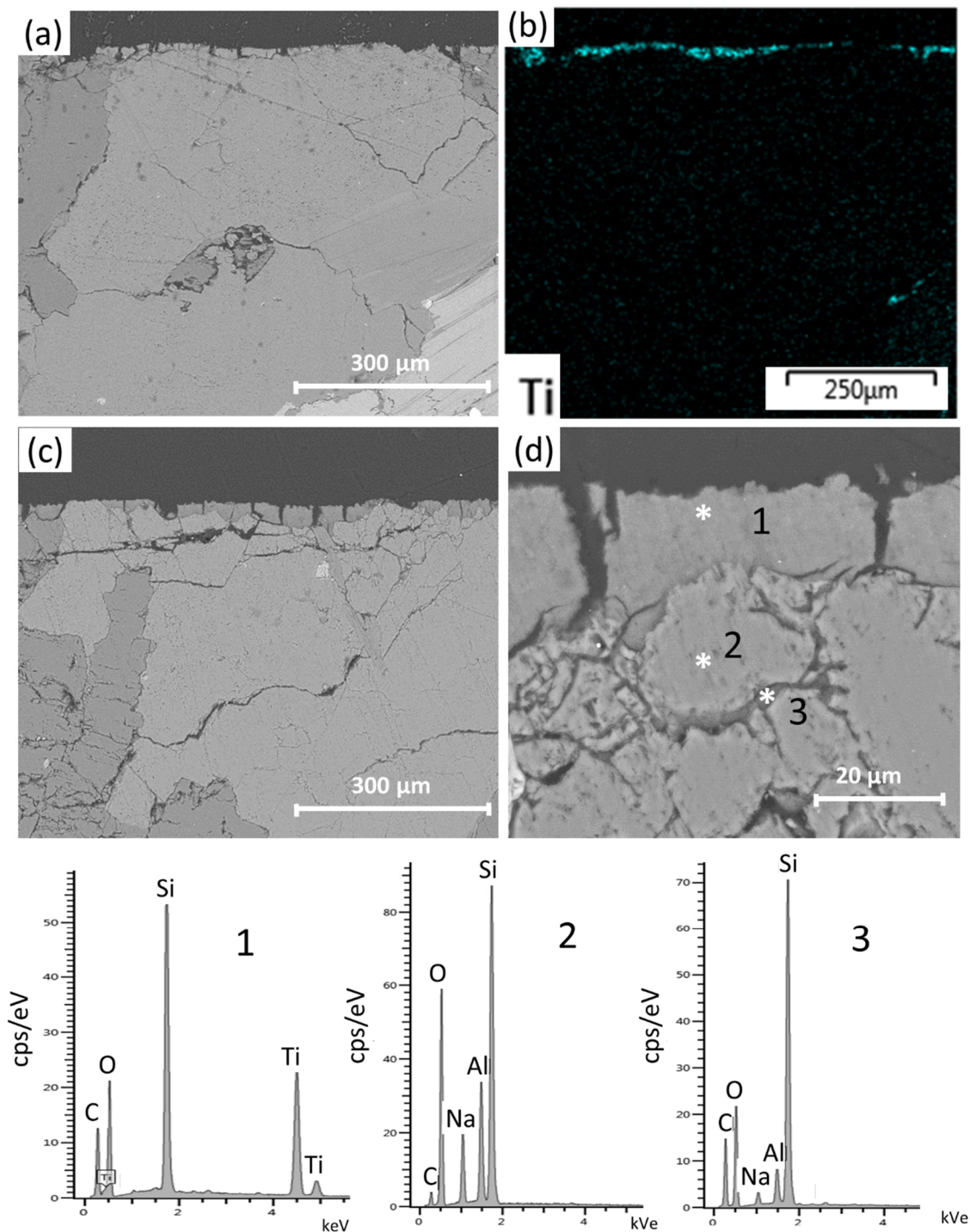
Figure 9. SEM micrographs of the polished cross sections from the surfaces treated with consolidant doped with 3 wt % of TiO$_2$ nanoparticles. (**a**) Estel 1000 treated surface. (**b**) Ti compositional map. (**c**,**d**): Nano Estel-treated surface, (d) is accompanied with the EDS spectra.

4. Discussion

In this manuscript the result of a comparative study between two different consolidants products applied on the Rodas granite commonly found in the heritage architecture from the NW Iberian Peninsula were shown. Considering the self-cleaning inferred by TiO$_2$ nanoparticles [16,47,48], they were added to consolidants with different compositions (Estel 1000: ethyl silicate and Nano Estel: nano-sized silica colloidal solution). However, as consolidants are commonly used in objects with

historic and artistic values, their application cannot infer aesthetic modifications, such as colorimetric changes [28]. In this sense, the influence of the TiO$_2$ nanoparticles content mixed with both consolidants on the appearance and the color of the granite was evaluated working with different nanoparticles concentration (0.5, 1, and 3 wt %). Therefore, the concentration thresholds for the TiO$_2$ addition without compromising the artistic historical value of each object were identified, i.e., the TiO$_2$ addition to the consolidant which did not induce changes in the appearance and color of the granite.

Considering the results obtained through spectrophotometry, only the nano-sized silica colloidal solution without TiO$_2$ nanoparticles did not induce a visible color change on the granite because for the rest of the samples, the global color changes (ΔE^*_{ab}) were higher than 3.5 CIELAB units, which is following [45], the threshold from which a color change is visible to a non-expert observer. La Russa et al. [13] applying the same consolidants on an ignimbrite detected also lower values of global color change on the Nano Estel coated surfaces than those for the Estel 1000 coated samples; specifically, they reported just negligible color modifications for the Nano Estel coated surfaces. Considering the consolidants without nanoparticles TiO$_2$, the ethyl silicate induced the highest global change (even in comparison with the consolidants doped with TiO$_2$) showing a ΔE^*_{ab} = 7.46 CIELAB units. This value was in agreement with the global color change found by Mosquera et al. [4] applying another tetraethoxysilane (Tegovakon V100 from Goldschmidt) in a similar granite. Moreover, de Rosario et al. [49] also applying Estel 1000 in a granitic sample found similar color changes. As a common trend due to the consolidant application on stones, bricks, etc. [2,49–52], in the samples coated without TiO$_2$ addition, a darkening and a yellowing were detected. Costa and Rodrigues [50] showed that dark minerals (biotite and iron forms mainly) in granite became darker and feldspar and plagioclase grains became more yellow with the ethyl silicate consolidant Wacker OH. In the current research, a notable darkening ($\Delta L^* > -7$ CIELAB units) and a slight increase of the yellowish coloration was detected on the surface coated with ethyl silicate; these changes were the responsible variations for the most intense global color change detected in this research. In the sample with nano-sized silica consolidant (without TiO$_2$), the darkening was less intense than that found in the ethyl silicate-coated sample; however, the yellowish increase was slightly higher. Despite the xerogel coating on the surface treated with ethyl silicate without TiO$_2$ was less extent (detected by SEM-EDS) than that found on the sample with the nano-silica suspension, the impact on the granite color of the former was more intense than that found on the surface coated with the ethyl silicate. This trend was also reported in other works [13,49]. It is important to highlight that several authors found that the darkening ($-\Delta L^*$) in volcanic rocks after the application of ethyl silicate consolidants often reverted to its original color in time or after artificial weathering [53,54]. Therefore, further studies about the tendency of the color of coated samples with TEOS in time should be performed.

SEM allowed the identification of a denser cracked xerogel coating on the surfaces with the nano-sized silica solution than that found on the ethyl silicate coated surfaces. Despite showing different extent degrees, both consolidants achieved superficial xerogel layers with fissures as commonly found in tetraethoxysilane products (TEOS) [49,55]. SEM observations of the cross sections confirmed: (i) a less compact layer on the surfaces treated with ethyl silicate comparatively to those with nano-silica solution; and (ii) a lower penetration rate through the fissures was detected in the surfaces with ethyl silicate. Zendri et al. [11] working with a colloidal silica consolidant and an ethyl silicate product on mortars also reported a greater penetration capacity of the colloidal silica, characterized by little particles comparatively to the ethyl silicate. Indeed, they measured that the superficial area of the nano-sized silica was about 150 m^2/g, while from ethyl silicate, the particle showed a superficial area about 10 m^2/g. As was reported in [41] the used nanoparticles showed a size of 30 nm. As consequence Zendri et al. [11] reported less cohesion effect of the ethyl silicate than that for the colloidal silica solution. In the current research, despite the same number of applications were performed regardless of the consolidant, the lower extent of the xerogel layer found on the Estel 1000 treated surface comparatively to that found on the Nano Estel treated surface, it might be related to the application procedure. Nano Estel (concentrated aqueous colloidal solution of nanoparticles silica) which is recommended

by the manufacturer to use at 30 vol % in water, considering the ruined substrates, it was applied directly on the granite, as was made by the Estel 1000 which is diluted in white spirit D40 (SiO_2 content of 30 wt %). It is important to indicate that the existence of the xerogel coatings could hinder the consolidation effectiveness because they could act as clogging layers. Although the consolidating effect has to be assessed in terms of penetration depths and variations on microstructural and mechanical properties [56], since the aim of this research was to determine the suitable TiO_2 concentrations added to the selected consolidants in order to inferred a self-cleaning property, further studies should be done on the consolidant effectiveness and self-cleaning of these surface xerogel coatings.

Different penetration rates for the consolidants without TiO_2 were detected by SEM using the polished cross sections: ~200 µm were detected in the Nano Estel treated surfaces while the penetration on the surface with Estel 1000 was almost negligible. Considering that the same number of applications was made for both consolidants, the different penetration rate might be dependent on: i) the application procedure, ii) the particle size of the silica particles, and iii) the solvent of the consolidant. As was reported previously, Nano Estel is a concentrated aqueous colloidal solution of nano-size silica particles that despite the manufacturer recommends its application at 30 vol % in distilled water, considering the ruined state of the heated granite, it was directly applied on the stone. Regarding the particle size, the nano-size silica particles (10–30 nm) might have allowed a better penetration into the finer pore structure of the granite (100–60 nm) than the TEOS. Considering the solvent of each consolidant, it should be considered that consolidant penetrates as far as the solvent [12]. The TEOS is diluted in white spirit (25 wt %) and nanosilica consolidant is based on an aqueous colloidal solution. Therefore, the faster solvent evaporation in the TEOS comparatively to the nano-silica suspension, will induce the low penetration. Franzoni et al. [56] working also with Estel 1000 on a limestone found that the amount of solvent evaporated between brush stroke was not negligible and therefore, the solvent evaporation conditions the final penetration and redistribution of the consolidant into the fissures.

The TiO_2 addition induced a reduction of the consolidant penetration, because regardless of the consolidant used, the TiO_2 nanoparticles were retained on the surface forming agglomerates with a length of about 60 µm, preventing their entry into fissures. In the samples with Estel 1000 and TiO_2, penetration was not detected, while in the Nano Estel coated surfaces, a penetration reduction of 90% was found comparatively to the surface coated without TiO_2 addition.

Attending to the aesthetical effect of the TiO_2 addition, regardless of the consolidant, the color data for the samples showed that the higher the TiO_2 content the higher the global color change. Comparing with the global color change detected on the coated samples without TiO_2, two different trends were found:

- On the one hand, in the samples coated with the ethyl silicate, the addition of the TiO_2 nanoparticles induced a reduction of the color change; the color of the coated samples with TiO_2 would be more similar to the coated stone without TiO_2 addition. However, using stereomicroscopy, it was found cracked white deposits into the superficial fissures of the granite; the higher the TiO_2 content, the higher the deposit extent on the surface. Therefore, as was reported in a previous article based on the use of the CIELAB parameters (as ΔE^*_{ab}) as indicator of the cleaning effectiveness [57], they have to be used with caution. In the current research, it has to be considered that the ethyl silicate by itself already generated an intense impact on the color of the stone. Therefore, it is important to study the quantitative results with the L-C^*_{ab} scatter plots.
- On the other hand, for surfaces coated with nano-sized silica suspension, the least TiO_2 content already induced a global color change higher than that found on the surface coated only with the consolidant. As was reported for the ethyl silicate samples, the higher the TiO_2 content, the broader the cracked white deposits.

Considering that for the low TiO_2 addition (0.5 wt %) the surface layers showed different texture, because in the samples with nano-silica consolidant, the sample showed a layer with an homogeneous nanoparticles distribution, while the mixture with ethyl silicate, white cracked deposits were found

again into the fissures and voids of the surface, different consolidant-TiO_2 nanoparticles interaction was found for lower TiO_2 concentrations.

In order to identify TiO_2 nanoparticle content thresholds for each consolidant in terms of an aesthetic point of view, it was identified that the addition of 0.5% TiO_2 in both consolidants already induced global color changes detected by an unexperienced observer [45], however it is necessary to interpret color results also from a conservation point of view [46]. Therefore, in the mixture of both consolidants with 0.5% TiO_2, as the ΔE^*_{ab} were lower than 5 CIELAB units, these changes imply a low to medium risk of incompatibility; i.e. these products can be considered as inducers of low to medium harmful effects of heritage elements. The rest of the compositions already induced high risks of incompatibility as products to be used in the conservation of cultural heritage elements, because their ΔE^*_{ab} were higher than five CIELAB units.

5. Conclusions

Appearance and colorimetric changes of the granite surfaces when consolidant products (Estel 1000: ethyl silicate and Nano Estel: nano-sized silica colloidal solution) were mixed with nanoparticles TiO_2 comparatively to the uncoated stone, were evaluated in this research. These variations suggested that the mixture of both consolidants with the minimal TiO_2 concentration tested (0.5 wt %), implied a low to medium risk of incompatibility, i.e., these products could induce low to medium harmful effects to heritage elements.

Attending to the effect on the surface, although high concentration of TiO_2 mixed with both consolidants induced cracked white deposits in fissures and voids detected on the surface, at the lower concentration (0.5% TiO_2) different patterns were detected: i) in the nano-sized silica consolidant, the nanoparticles TiO_2 were kept as a suspension after the polymerization (showing narrower fissures than those found in the superficial coatings with higher TiO_2 concentrations); and ii) in ethyl silicate consolidant, the nanoparticles TiO_2 induced cracked white deposits filling the fissures and voids as was identified for the consolidant layers with higher TiO_2 contents. The higher the concentration, the more visible the nanoparticle accumulation on the surface of the stone.

Considering the penetration depth achieved by the different products, higher penetration rates were identified in the granite coated with nano-sized silica colloidal solution, while ethyl silicate was only found in the few first μm. Therefore, penetration depends on the application procedure, the solvent of the consolidant and the silica particle size. The TiO_2 addition seemed to reduce the penetration of the nano-sized silica consolidant. TiO_2 nanoparticles were kept on the surface forming agglomerates while consolidant product without TiO_2 was found covering mineral grains in the first μm of the stone coated with the nano-sized silica consolidant.

The trend of the color change due to the mixture of the product with the TiO_2 nanoparticles was different considering the consolidant compositions. TiO_2 addition to ethyl silicate induced an increase of the color changes comparatively to the effect of the consolidant without TiO_2 nanoparticles on the stone, while the nano-sized silica suspension caused a reduction of the color changes comparatively to that found in the surface coated without TiO_2. In this sense, it seems suitable to perform a study on the color evolution of these consolidants in time.

For further researchers, two different research lines might be designed. On the one hand, it seems necessary to study the influence of the TiO_2 addition on the consolidating effect of the product considering the superficial adherence and the distribution of the product through the fissure system of the granite. On the other hand, further research should be based on: i) the self-cleaning property of the coated surfaces in order to decompose real engine soot; and ii) the biocidal effect due to the addition of TiO_2 nanoparticles to the consolidant products.

References

1. ICOMOS. *Ilustrated Glossary on Stone Deterioration Patterns. Monuments and Sites*; XVICOMOS-ICS; ICOMOS: Paris, France, 2008.
2. Wheeler, G. *Alkoxysilanes and the Consolidation of Stone*; The Getty Conservation Institute: Los Angeles, CA, USA, 2005; p. 215.
3. Mosquera, M.J.; Pozo, J.; Esquivias, L. Stress during Drying of Two Stone Consolidants Applied in Monumental Conservation. *J. Sol-Gel Sci. Technol.* **2003**, *26*, 1227–1231. [CrossRef]
4. Mosquera, M.J.; Santos, D.M.D.L.; Rivas, T.; Sanmartín, P.; Silva, B. New Nanomaterials for Protecting and Consolidating Stone. *J. Nano Res.* **2009**, *8*, 1–12. [CrossRef]
5. Scherer, G.W. Recent progress in drying of gels. *J. Non-Cryst. Solids* **1992**, *147*, 363–374. [CrossRef]
6. Mosquera, M.J.; Bejarano, M.; De La Rosa-Fox, N.; Esquivias, L. Producing Crack-Free Colloid−Polymer Hybrid Gels by Tailoring Porosity. *Langmuir* **2003**, *19*, 951–957. [CrossRef]
7. Brush, J.; Kotlik, P. Cracking of organosilicone stone consilidants in gel form. *Stud. Conserv.* **1996**, *41*, 55–59. [CrossRef]
8. Xu, F.; Zeng, W.; Li, D. Recent advance in alkoxysilane-based consolidants for stone. *Prog. Org. Coat.* **2019**, *127*, 45–54. [CrossRef]
9. Fernández, A.S.; Gomez-Villalba, L.S.; Rabanal, M.E.; Fort, R. New nanomaterials for applications in conservation and restoration of stony materials: A review. *Materiales de Construcción* **2017**, *67*, 107. [CrossRef]
10. Zornoza-Indart, A.; Lopez-Arce, P. Silica nanoparticles (SiO2): Influence of relative humidity in stone consolidation. *J. Cult. Herit.* **2016**, *18*, 258–270. [CrossRef]
11. Zendri, E.; Biscontin, G.; Nardini, I.; Riato, S. Characterization and reactivity of silicatic consolidants. *Constr. Build. Mater.* **2007**, *21*, 1098–1106. [CrossRef]
12. Falchi, L.; Balliana, E.; Izzo, F.; Agostinetto, L.; Zendri, E. Distribution of nanosilica dispersions in Lecce stone. *Sci. Ca´Foscari* **2013**, *1*, 40–46.
13. La Russa, M.F.; Ruffolo, S.A.; Rovella, N.; Belfiore, C.M.; Pogliana, P.; Pelosi, C.; Andaloro, M.; Crisci, G.M. Cappadocian ignimbrite cave churches: Stone degradation and conservation strategies. *Period. Mineral.* **2014**, *83*, 187–206.
14. Kapridaki, C.; Pinho, L.; Mosquera, M.J.; Maravelaki, P.N. Producing photoactive, transparent and hydrophobic SiO2-crystalline TiO2 nanocomposites at ambient conditions with application as self-cleaning coatings. *Appl. Catal. B Environ.* **2014**, *156*, 416–427. [CrossRef]
15. Colangiuli, D.; Calia, A.; Bianco, N. Novel multifunctional coatings with photocatalytic and hydrophobic properties for the preservation of the stone building heritage. *Constr. Build. Mater.* **2015**, *93*, 189–196. [CrossRef]
16. Pant, B.; Park, M.; Park, S.J. Recent Advances in TiO_2 Films Prepared by Sol-Gel Methods for Photocatalytic Degradation of Organic Pollutants and Antibacterial Activities. *Coatings* **2019**, *9*, 613. [CrossRef]
17. Fonseca, A.J.; Pina, F.; Macedo, M.F.; Leal, N.; Romanowska-Deskins, A.; Laiz, L.; Gómez-Bolea, A.; Saiz-Jimenez, C. Anatase as an alternative application for preventing biodeterioration of mortars: Evaluation and comparison with other biocides. *Int. Biodeterior. Biodegrad.* **2010**, *64*, 388–396. [CrossRef]
18. Munafò, P.; Goffredo, G.B.; Quagliarini, E. TiO2-based nanocoatings for preserving architectural stone surfaces: An overview. *Constr. Build. Mater.* **2015**, *84*, 201–218. [CrossRef]
19. Pozo-Antonio, J.; Dionísio, A. Self-cleaning property of mortars with TiO_2 addition using real diesel exhaust soot. *J. Clean. Prod.* **2017**, *161*, 850–859. [CrossRef]

20. Pant, B.; Barakat, N.A.M.; Pant, H.R.; Park, M.; Saud, P.S.; Kim, J.-W.; Kim, H.-Y. Synthesis and photocatalytic activities of CdS/TiO$_2$ nanoparticles supported on carbon nanofibers for high efficient adsorption and simultaneous decomposition of organic dyes. *J. Colloid Interface Sci.* **2014**, *434*, 159–166. [CrossRef]

21. Pant, B.; Park, M.; Park, S.-J. Hydrothermal synthesis of Ag$_2$CO$_3$-TiO$_2$ loaded reduced graphene oxide nanocomposites with highly efficient photocatalytic activity. *Chem. Eng. Commun.* **2019**, 1–8. [CrossRef]

22. Fujishima, A.; Zhang, X.T.; Tryk, D.A. TiO$_2$ photocatalysis and related surface phenomena. *Surf. Sci. Rep.* **2008**, *63*, 515–582. [CrossRef]

23. Allen, N.S.; Mahdjoub, N.; Vishnyakov, V.; Kelly, P.J.; Kriek, R.J. The effect of crystalline phase (anatase, brookite and rutile) and size on the photocatalytic activity of calcined polymorphic titanium dioxide (TiO$_2$). *Polym. Degrad. Stab.* **2018**, *150*, 31–36. [CrossRef]

24. Graziani, L.; Quagliarini, E.; D'Orazio, M. TiO2-treated different fired brick surfaces for biofouling prevention: Experimental and modelling results. *Ceram. Int.* **2016**, *42*, 4002–4010. [CrossRef]

25. Quagliarini, E.; Bondioli, F.; Goffredo, G.B.; Cordoni, C.; Munafò, P. Self-cleaning and de-polluting stone surfaces: TiO 2 nanoparticles for limestone. *Constr. Build. Mater.* **2012**, *37*, 51–57. [CrossRef]

26. Smits, M.; Chan, C.K.; Tytgat, T.; Craeye, B.; Costarramone, N.; Lacombe, S.; Lenaerts, S. Photocatalytic degradation of soot deposition: Self-cleaning effect on titanium dioxide coated cementitious materials. *Chem. Eng. J.* **2013**, *222*, 411–418. [CrossRef]

27. Cohen, J.D.; Sierra-Gallego, G.; Tobón, J. Evaluation of Photocatalytic Properties of Portland Cement Blended with Titanium Oxynitride (TiO2−xNy) Nanoparticles. *Coatings* **2015**, *5*, 465–476. [CrossRef]

28. Venice Charter, 1964. The Venice Charter for the Conservation and Restoration of Monuments and Sites, 1964. Available online: http://www.icomos.org/venicecharter2004/index.html (accessed on 6 January 2020).

29. IGME (Instituto Geológico y Minero de España). *Mapa Geológico de España*, 2nd ed.; Serie Magna. E 1:50000, Hoja 224-Ponteareas; Spanish Government: Madrid, Spain, 1981.

30. Capdevila, R.; Floor, P. Les differents types de granites hercyniens et leur distribution dans le Nord-Ouest de l'Espagne. *Bol. Geol. Min.* **1970**, *81*, 215–225.

31. Escuder, J.; Carbonell, R.; Martí, D.; Pérez-Estaún, A. Interacción fluido-roca a lo largo de las superficies de fractura: Efectos mineralógicos y texturales de las alteraciones observadas en el Plutón Granítico de Albalá, SO del Macizo Hercínico Ibérico. *Boletín Geológico y Minero* **2001**, *112*, 59–78.

32. Fernandez-Caliani, J.C.; Galán, E.; Aparicio, P.; Miras, A.; Márquez, M.; Fernández, P.A. Origin and geochemical evolution of the Nuevo Montecastelo kaolin deposit (Galicia, NW Spain). *Appl. Clay Sci.* **2010**, *49*, 91–97. [CrossRef]

33. RILEM (Réunion Internationale des Laboratoires d'Essais et de Recherche sur les Matériaux et les Constructions). *Commission 25 PEM. Protection Et Erosion Des Monuments. Recommandations Provisoires. Essais Recommande´S Pour Mesurer L'altération Des Pierres Et Évaluer L'efficacité Des Méthodes De Traitement. Test No. II. 1: Open porosity*; RILEM: Paris, France, 1980. (In French)

34. De Rosario, I. Eficacia de Consolidantes e Hidrofugantes de Nueva Síntesis en Rocas Graníticas Optimización de Métodos de Evaluación. Ph.D. Thesis, University of Vigo, Pontevedra, Spain, 2017.

35. Winkler, E.M. *Stone: Properties, Durability in Man's Environment*; Springer: Berlin, Germany, 1975.

36. Pozo-Antonio, J.S.; Rivas, T.; Carrera, F.; García, L. Deterioration processes affecting prehistoric rock art engravings in granite in NW Spain. *Earth Surf. Process. Landf.* **2018**, *43*, 2435–2448. [CrossRef]

37. Rivas, T.; Pozo-Antonio, J.S.; Ramil, A.; López, A.J. Influence of the weathering rate on the response of granite to nanosecond UV laser irradiation. *Sci. Total Environ.* **2020**, *706*, 135999. [CrossRef]

38. Calvo, R.M.; García-Rodeja, E.; Macias, F. Mineralogical variability in weathering microsystems of a granitic outcrop of Galicia (Spain). *CATENA* **1983**, *10*, 225–236. [CrossRef]

39. Taboada, T.; García, C. Pseudomorphic transformation of plagioclases during the weathering of granitic rocks in Galicia (NW Spain). *Catena* **1999**, *35*, 291–302. [CrossRef]

40. CTS España S.L (Web). Available online: https://shop-espana.ctseurope.com/ (accessed on 10 December 2019).

41. Pozo-Antonio, J.S.; Dionísio, A. Physical-mechanical properties of mortars with addition of TiO2 nanoparticles. *Constr. Build. Mater.* **2017**, *148*, 261–272. [CrossRef]

42. Evonik Resource Efficiency GmbH (Web). Available online: https://corporate.evonik.com/en/company/segments/resource-efficiency/ (accessed on 10 December 2019).

43. *CIE S014-4/E: 2007. Colorimetry Part 4: CIE 1976 L*a*b* Colour Space*; Commission Internationale de l'eclairage, CIE Central Bureau: Vienna, Austria, 2007.

44. Prieto, B.; Sanmartín, P.; Silva, B.; Martinez-Verdú, F. Measuring de the color of granite rocks. A proposed procedure. *Color Res. Appl.* **2010**, *35*, 368–375. [CrossRef]

45. Mokrzycki, W.; Tatol, M. Color difference DeltaE-A survey. *Mach. Graph. Vis.* **2011**, *20*, 383–411.

46. Rodrigues, J.D.; Grossi, A. Indicators and ratings for the compatibility assessment of conservation actions. *J. Cult. Herit.* **2007**, *8*, 32–43. [CrossRef]

47. Beydoun, D.; Amal, R.; Low, G.; McEvoy, S. Role of Nanoparticles in Photocatalysis. *J. Nanoparticle Res.* **1999**, *1*, 439–458. [CrossRef]

48. La Russa, M.F.; Ruffolo, S.A.; Rovella, N.; Belfiore, C.M.; Palermo, A.M.; Guzzi, M.T.; Crisci, G.M. Multifunctional TiO$_2$ coatings for Cultural Heritage. *Prog. Org. Coatings* **2012**, *74*, 186–191. [CrossRef]

49. De Rosario, I.; Elhaddad, F.; Pan, A.; Benavides, R.; Rivas, T.; Mosquera, M.J. Effectiveness of a novel consolidant on granite: Laboratory and in situ results. *Constr. Build. Mater.* **2015**, *76*, 140–149. [CrossRef]

50. Costa, D.; Rodrigues, J.D. Assessment of color changes due to treatment products in heterochromatic stones. In *The Conservation of Granitic Rocks*; Rodrigues, J.D., Costa, D., Eds.; LNEC: Lisbon, Portugal, 1996; pp. 95–101.

51. Pinto, A.P.F.; Rodrigues, J.D. Impacts of consolidation procedures on color and absorption kinetics of carbonate stones. *Stud. Conserv.* **2014**, *59*, 79–90. [CrossRef]

52. Cultrone, G.; Ibáñez, V.M.S. Consolidation with ethyl silicate: How the amount of product alters the physical properties of the bricks and affects their durability. *Materiales de Construcción* **2018**, *68*, 173. [CrossRef]

53. Nishiura, T. Laboratory test on the color change of stone by impregnation with silane. In *Preprints of the Eighth Triennial Meeting in Sydney (Australia) by ICOM Committee for Conservation*; Grimstad, K., Ed.; Getty Conservation Institute: Los Angeles, CA, USA, 1987; pp. 509–512.

54. Wheeler, G.; Newman, R. Analysis and treatment of a stone urn from the Imperial Hotel, Tokyo. In *Lavas and Volcanic Tuffs*; Charola, A.E., Koestler, R.J., Lombardi, G., Eds.; ICCROM: Rome, Italy, 1994; pp. 157–161.

55. Brinker, C.J.; Scherer, G.W. *Sol-Gel Science*; Academic Press: New York, NY, USA, 1990.

56. Franzoni, E.; Grazani, G.; Sassini, E.; Bacilieri, G.; Griffa, M.; Lura, P. Solvent-based ethyl silicate for stone consolidation: Influence of the application technique on penetration depth, efficacy and pore occlusion. *Mater. Struct.* **2015**, *48*, 3503–3515. [CrossRef]

57. Pozo-Antonio, J.S.; Rivas, T.; Fiorucci, M.P.; López, A.J.; Ramil, A. Effectiveness and harmfulness evaluation of graffiti cleaning by mechanical, chemical and laser procedures on granite. *Microchem. J.* **2016**, *125*, 1–9. [CrossRef]